BULLETIN OF THE POLISH ACADEMY OF SCIENCES
TECHNICAL SCIENCES, Vol. 73(4), 2025, Article number: e153841
DOI: 10.24425/bpasts.2025.153841

Energy efficiency of supercapacitors in hybrid energy storage systems

Mirosław LEWANDOWSKI*, Marek ORZYŁOWSKI, and Tadeusz MACIOŁEK

Electrical Power Engineering Institute of the Warsaw University of Technology, Warsaw, Poland

Abstract. The supercapacitor supports the main energy source of the hybrid electrical energy storage system. In short periods, it supplies additional energy or absorbs braking energy. The paper addresses the issue of energy losses in supercapacitors used in such a pulsed mode of operation. Commonly used first-order RC capacitor impedance models are not a good basis for accurate calculation results of energy losses in supercapacitors. The article presents fractional-order supercapacitor impedance models based on the Cole-Cole relaxation equation. The following part presents the results of measurements of energy losses in real supercapacitors in comparison with simulation calculations using both above-mentioned supercapacitor impedance models. The article also discusses the problem of using the equivalent series resistance (ESR) values in RC impedance models, called AC ESR and DC ESR, specified by different supercapacitor manufacturers. It shows that the simulation results using the presented fractional impedance model are the closest to reality. The use of the other discussed models leads to even a several-fold underestimation of energy losses in supercapacitors used in electric energy storage systems.

Keywords: supercapacitor; storage system; energy loss; fractional calculus; impedance model.

1. INTRODUCTION

Supercapacitors are essential elements of hybrid energy storage systems for electric vehicles and electric microgrids. Due to their power density, which significantly exceeds the power density of batteries and fuel cells [1], they provide an efficient energy supply during vehicle acceleration and energy absorption during braking, e.g., [2–4]. In microgrids, the supercapacitors enable stabilization of the parameters of these networks during sudden changes in power demand and during fuel cell activation. Due to increasing demand, global production of supercapacitors is also systematically increasing.

Designing a hybrid energy storage system requires determining its electrical efficiency and thermal losses during operation. Among other things, it is necessary to correctly determine the thermal losses of supercapacitors and the effect of losses on their temperature and the temperature of the main energy source, which is usually a lithium-ion battery. One of the important reasons is that overheated lithium-ion batteries can be damaged or even cause a fire that is difficult to extinguish.

Determining the losses of supercapacitors in different cases of their power load is facilitated by the simulation of their electrical states using accurate models of supercapacitor impedance. As demonstrated in this paper, among others, a simple first-order RC model is insufficient for supercapacitors in this case. A more accurate description of supercapacitor impedance can be obtained using various configurations of multi-element RC equivalent circuits. A review of such models, created on the basis of integer differential equations, is presented, among others, by [5–7]. The identification of the values of the parameters of these models is, however, quite difficult due to their large number. Another way of modelling the impedance of supercapacitors is the use of fractional-order differential equations. Fractional-order models of supercapacitor impedance based on the Cole-Cole [8] and the Cole-Davidson [9] dielectric relaxation equations, describe quite accurately the dynamic properties of supercapacitors using a relatively small number of parameters. The proposal of such models for supercapacitors was presented in [10] and developed in e.g. [11–14]. Work is also being conducted on other fractional order models based on the use of the constant phase elements (CPE) with their review presented, e.g., in [15, 16]. However, these types of simple models with a single CPE have a significant limitation resulting from the fact that this element determines the phase shift for low frequencies. A real supercapacitor has a phase shift for these frequencies tending to achieve -90° (Fig. 4 and Fig. 5), which is close to the phase shift of an ideal capacitor.

The use of models based on fractional differential equations for various purposes is widely described in the available literature. The fundamentals and application of such models for control purposes are discussed in some detail in the monograph [17], among others. Energy losses in supercapacitors are usually treated marginally for these models. For example, in the monograph on electrical energy storage systems [18], in the examples of calculating the charging and discharging efficiency of a supercapacitor, only the model of its impedance in the form of a first-order RC circuit is used. These considerations are valid only for a constant current load. Meanwhile, it should be considered that in the energy storage systems energy losses of a supercapacitor occur mainly during pulse operation.

When needed, the supercapacitor supplies additional energy directly to the load of the energy storage system or absorbs it

*e-mail: Miroslaw.Lewandowski@ee.pw.edu.pl

Manuscript submitted 2024-09-03, revised 2024-12-29, initially accepted for publication 2025-02-18, published in July 2025.

from the load. This happens in short periods. Between these periods, the control system of the storage system prepares the supercapacitor state of charge for the expected role. For example, when the vehicle is stationary, its acceleration is expected, so the supercapacitor is charged from the main source of energy. On the other hand, when the vehicle is at high speed, it is discharged to the main source of energy to be able to absorb braking energy. The periods during which energy flows between the supercapacitors and the main energy source are much longer than the periods during which energy flows between the supercapacitor and the energy storage system load. As a result, the preparation of the supercapacitor state of charge takes place using a much smaller current.

The flow of electric charge Q_x during the time T_x requires the current

$$I_x = \frac{Q_x}{T_x}. \tag{1}$$

When current I_x flows through an element with resistance R_x is lost energy

$$E_x = I_x^2 R_x T_x = \left(\frac{Q_x}{T_x}\right)^2 R_x T_x = \frac{Q_x^2 R_x}{T_x}. \tag{2}$$

As a result, during the above-mentioned state of charge preparation, there are small energy losses in the equivalent series resistance (ESR) of the supercapacitor compared to the direct energy supply to the load. For this reason, the paper focuses on the energy losses during its transfer between the supercapacitor and the load.

The paper discusses the application of fractional-order supercapacitor impedance models to calculate losses during pulse operation, corresponding to their application in energy storage systems. These results are compared with the results of loss calculations based on widely used first-order RC models.

2. SUPERCAPACITOR IMPEDANCE MODELS

The simplest model of a real capacitor impedance is a series connection of the ideal capacitance C_0 and the equivalent series resistance R_{ESR}. This resistance can be the basis for calculating energy losses occurring in a real capacitor. The above parameters are also provided by manufacturers as basic technical data of supercapacitors. However, it should be emphasized that the ESR of supercapacitors is specified in catalogs as AC ESR and DC ESR. The commonly used value of the resistive part of the capacitor impedance at a frequency of 1 kHz is given as AC ESR. On the other hand, the DC ESR value refers to the results of measurements according to the method specified in the IEC 62391-1:2022 standard [19] or its modifications. In this article, the considerations are initially based on models using AC ESR, denoted R_C.

The impedance Z_{RC1} (RC1 model), which is a series connection of the capacitance C_0 and the resistance R_C, is described by the relationship using the Laplace transformation

$$Z_{\mathrm{RC1}} = \frac{1}{sC_0} + R_C = Z_1 + Z_2, \tag{3}$$

where

$$Z_1 = \frac{1}{sC_0}, \tag{4}$$

$$Z_2 = R_C. \tag{5}$$

By replacing the Laplace transform with the Fourier transform in the equations, i.e., in effect replacing the operator s with the operator $j\omega$, the frequency response of the impedance can be determined.

Equation (3) is useful as a mathematical model for loss calculation in common capacitors. Studies show that the frequency characteristics of supercapacitor impedances differ significantly from the characteristics of models described by equation (3). This issue is described extensively in more detail in the literature. One solution to this problem may be the impedance represented as a quotient of integer-order polynomials of s, related to complex RC ladder circuits, e.g., [5–7]. Another approach can be to build a model based on a mathematical model of the physical phenomena occurring in supercapacitors. This leads to fractional order models, among other things. A comparison of different models of integer-order and fractional-order supercapacitor impedance is presented, for example, in [12].

The capacitance of a supercapacitor is related to the electrical double layer that forms at the interface between the electrodes and the electrolyte. The permittivity of this layer can be described by the Debye equation. However, in practice, it is better described by modified dielectric relaxation equations [20, 21, 24]. One such equation is the Havriliak-Negami model, i.e.,

$$\varepsilon_{HN}(j\omega) = \varepsilon_\infty + \frac{\varepsilon_s - \varepsilon_\infty}{\left[1 + (j\omega T)^\delta\right]^\gamma}, \quad 0 < \delta \le 1, \quad 0 < \gamma \le 1, \tag{6}$$

where ω – angular frequency, ε_∞ – permittivity at the high frequency bound, ε_s – static, low-frequency permittivity, T – the characteristic relaxation time, γ, δ – coefficients chosen empirically.

Assuming the conditions $\gamma = 1$ and $\delta < 1$ from equation (6) we obtain the Cole-Cole [8] model

$$\varepsilon_{CC}(j\omega) = \varepsilon_\infty + \frac{\varepsilon_s - \varepsilon_\infty}{1 + (j\omega T)^\delta}, \quad 0 < \delta < 1, \tag{7}$$

while for $\gamma < 1$ and $\delta = 1$ we obtain the Cole-Davidson model [20]

$$\varepsilon_{CD}(j\omega) = \varepsilon_\infty + \frac{\varepsilon_s - \varepsilon_\infty}{(1 + j\omega T)^\gamma}, \quad 0 < \gamma < 1. \tag{8}$$

The models described by equations (6), (7) and (8) are fractional-order models. The Debye equation is obtained for $\delta = 1$ and $\gamma = 1$.

In the Debye equation the characteristic relaxation time T determines the return time of a perturbed system into equilibrium after changing the applied electric field. In equations (6), (7), and (8) discussed here; however, it becomes a formal parameter,

because when raised to a fractional power it loses its physical meaning. Because in the impedance of a supercapacitor, the ESR has a significant value R_C and there is a dependence $\varepsilon_s \gg \varepsilon_\infty$, in further considerations, it can be assumed that $\varepsilon_\infty = 0$.

In fractional order models equations (6), (7), and (8) there are exponents δ and γ with values selected experimentally. The reason for this approach is that in these cases, fractional models with relatively simple structures describe a series of complex physical processes occurring in the entire volume of supercapacitors. Voltage, as a state variable of the model, concerns the supercapacitor terminals, while physical phenomena inside are related to the electric field generated by ions adhering to the porous surfaces of electrodes and moving between these electrodes [22], among others. Their movement depends on the viscosity of the electrolyte [23] in which the ions surrounded by solvent molecules move. The ratio of the pore size in the electrodes to the size of the ions is also important for the movement of ions.

In studies, for example in [10], it was shown that the model based on the Cole-Davidson equation (6) approximates the frequency response of the impedance of a real supercapacitor much better than the model equation (3). The paper [11] argues that for approximating these characteristics it is more advisable to use the Cole-Cole dielectric relaxation equation [8]. This leads to obtaining a fractional impedance equation of canonical form [17]

$$Z(s) = \frac{b_0 s^{\beta_0} + b_1 s^{\beta_1} + \ldots + b_{m-1} s^{\beta_{m-1}} + b_m s^{\beta_m}}{a_0 s^{\alpha_0} + a_1 s^{\alpha_1} + \ldots + a_{n-1} s^{\beta_{n-1}} + a_n s^{\alpha_n}}. \tag{9}$$

It is worth mentioning that the supercapacitor leakage resistance is so large that it does not affect the change in the supercapacitor voltage in the considered time horizon of the pulse operation in the energy storage system. The supercapacitor impedance model, based on the Cole-Cole equation (CC model), can then be written as [11]

$$\begin{aligned} Z_{CC} &= \frac{1}{s\dfrac{C_0}{1+(sT)^\delta}} + R_C = \frac{1 + s^\delta T^\delta + sR_C C_0}{sC_0} \\ &= \frac{1}{sC_0} + \frac{T^\delta}{s^{1-\delta} C_0} + R_c = Z_1 + Z_3 + Z_2, \end{aligned} \tag{10}$$

where

$$Z_3 = \frac{T^\delta}{s^{1-\delta} C_0}. \tag{11}$$

The Z_3 term is an additional term that does not appear in equation (3).

The general form of the transfer function equation (9), including the impedance, is related to fractional calculus [17]. One of the definitions of a fractional derivative of α-order is the Caputo definition

$${}_cD_t^\alpha f(t) = \frac{1}{\Gamma(n-\alpha)} \int_c^t \frac{f^{(n)}(\tau)}{(t-\tau)^{\alpha-n+1}} \mathrm{d}\tau, \tag{12}$$

where $n-1 < \alpha < n$, $n \in N$. It facilitates, for example, the determination of the Laplace transform of fractional differential equations [24]. It is worth noting that when using the relationships given in the literature related to the fractional Laplace transform, one should avoid mistakes related to the initial states [25].

In the case of time response simulations, all preceding states must be considered, starting from the previous steady state. For the simulation, one can use the Grünwald-Letnikov definition of the fractional derivative

$${}_cD_t^\alpha f(t) = \lim_{h\to 0} h^{-\alpha} \sum_{j=0}^{\left\lfloor \frac{t-a}{h} \right\rfloor} w_j^{(\alpha)} f(t-jh), \tag{13}$$

where $\left\lfloor \dfrac{t-a}{h} \right\rfloor$ denotes the integer part of the quotient. Because of its reference to the time step h, it is naturally suited to numerical calculations using a computer. The values of $w_j^{(\alpha_i)}$ can be calculated based on the iterative relationship

$$w_0^{(\alpha)} = 1, \quad w_j^{(\alpha)} = \left(1 - \frac{\alpha+1}{j}\right) w_{j-1}^{(\alpha)}, \quad j = 1,2,3,\ldots \tag{14}$$

The problem of complications when using the given definitions of fractional derivatives can be easily solved in practice by using appropriate computational tools, e.g., the FOTF toolbox [26], which comes with the MATLAB software. These tools are equivalent to those contained in the MATLAB control toolbox for integer-order systems.

The dynamic properties of the impedance model equation (10), which are different from those of model equation (3), can briefly describe their voltage responses to current steps. The voltage response U_{RC1} of impedance equation (3) to a current step of value I_A is the sum of two terms, which are inverse Laplace transforms of Z_1 and Z_2 multiplied by the transform of step. The term associated with Z_1 has the form of a linear increase

$$U_{1A} = \mathscr{L}^{-1}\left[\frac{I_A}{s} Z_1\right] = \mathscr{L}^{-1}\left[\frac{I_A}{s^2 C_0}\right] = t\frac{I_A}{C_0} 1(t), \tag{15}$$

and the one associated with the Z_2 is the step

$$U_{2A} = \mathscr{L}^{-1}\left[\frac{I_A}{s} Z_2\right] = \mathscr{L}^{-1}\left[\frac{I_A}{s} R_C\right] = I_A R_C 1(t). \tag{16}$$

In the case of impedance equation (10), the voltage U_{CC} is a sum of responses in equation (15) and equation (16) with the addition of the nonlinear term [17]

$$\begin{aligned} U_{3A} &= \mathscr{L}^{-1}\left[\frac{I_A}{s} Z_3\right] = \mathscr{L}^{-1}\left[\frac{I_A T^\delta}{s^{2-\delta} C_0}\right] \\ &= t^{1-\delta} \frac{I_A T^\delta}{C_0 \Gamma(2-\delta)} 1(t). \end{aligned} \tag{17}$$

Let us consider a rectangular input current pulse of amplitude 1 A and duration 1 s, which can be treated as the sum of two steps of opposite polarity, shifted in time by 1 s. The voltage responses are the superposition of the responses to both steps.

The responses to the impulse of terms Z_1, Z_2, and Z_3 and the summary responses of equation (3) and equation (10) are shown in Fig. 1. It is worth noting that the impedance equation (10), which is related to the supercapacitor terminals, shows voltage changes even after the current forcing ceases. This is due to dynamic phenomena occurring inside the supercapacitor. The above phenomenon creates a certain problem related to the identification of model parameters. The authors of the article identified the parameters of the model equation (10) for different supercapacitors using two methods. One of them assumed the best approximation of the frequency characteristics of the supercapacitor impedance by the characteristics of its model [11]. The second method led to the best approximation of the voltage response to the same current excitations. For this purpose, the least squares method was used. The identification results of both methods differ slightly.

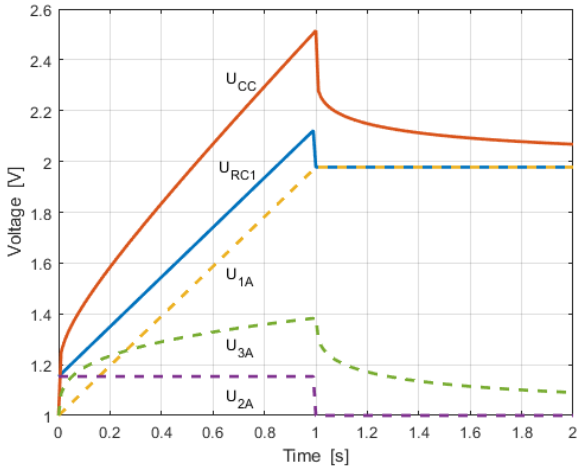

Fig. 1. Voltage responses of RC1 and CC models of 1 F supercapacitor to 1 A current pulse

The reason for this difference is as follows. Before their determination of the supercapacitor impedance model parameters by the time method, a statically steady state is maintained. However, in the case of frequency identification, at the moment of starting the identification, there is a state that is established dynamically as a result of long-term stimulation with a sinusoidal current wave of a specific frequency. It is also evident that the results of the identification of parameters of supercapacitor impedance models by the time method depend on the shape and length of the pulses, and therefore on their frequency spectrum, which is usually limited. Thus, despite its imperfections, the frequency identification method, conducted in a wide frequency range of 1 mHz – 1 kHz, seems to be the most appropriate.

The graphs of the frequency and time responses and data in the tables presented in this article are the results of the authors' research conducted in the laboratory of the Warsaw University of Technology. The laboratory equipment is shown in Fig. 2. In general, the tests concern many types of supercapacitors from different manufacturers, as exemplified by Fig. 3.

Figures 4 and 5 present comparisons of measurement results of the frequency characteristics of supercapacitor impedances

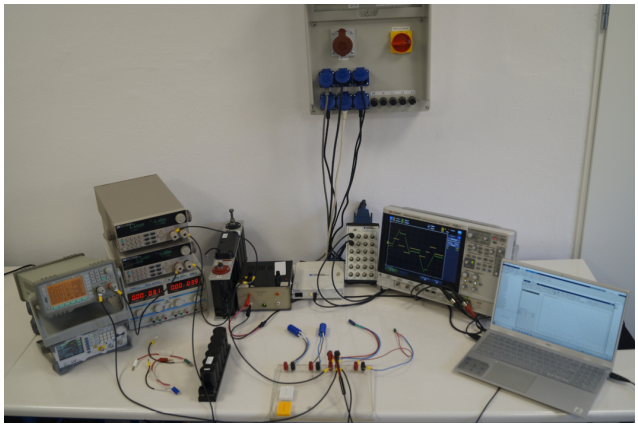

Fig. 2. Supercapacitor laboratory equipment at the Warsaw University of Technology

Fig. 3. Examples of supercapacitors under tests at the Warsaw University of Technology

and their approximation by the RC1 and CC impedance models. The measurement results of the frequency characteristics of the real supercapacitors are presented as points, while the characteristics of the fractional model equation (10) are presented as continuous lines. The characteristics of the corresponding RC1 models are presented as dashed lines. The impedance magnitude graphs in Fig. 4 and Fig. 5 are presented on a double-logarithmic scale, while the phase angle graph is linear with a logarithmic frequency scale.

As can be seen in Fig. 4 and Fig. 5, the fractional impedance model CC approximates the real impedance magnitude and phase graphs much better than the RC1 model. The presented graphs show extreme cases in which the differences between the two discussed impedance models are relatively large and relatively small. For the supercapacitor with the frequency response in Fig. 4, the influence of the Z_3 term in its impedance model on the time response is more significant than in the case of the supercapacitor with the frequency response in Fig. 5. Both pre-

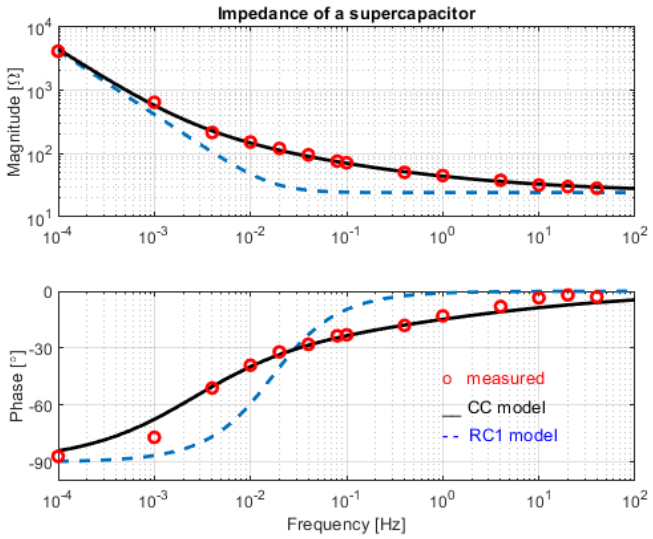

Fig. 4. Frequency characteristics of the impedance of the 0.33 F supercapacitor: measurement results – circles, fractional CC model – continuous line, RC1 model – dashed line

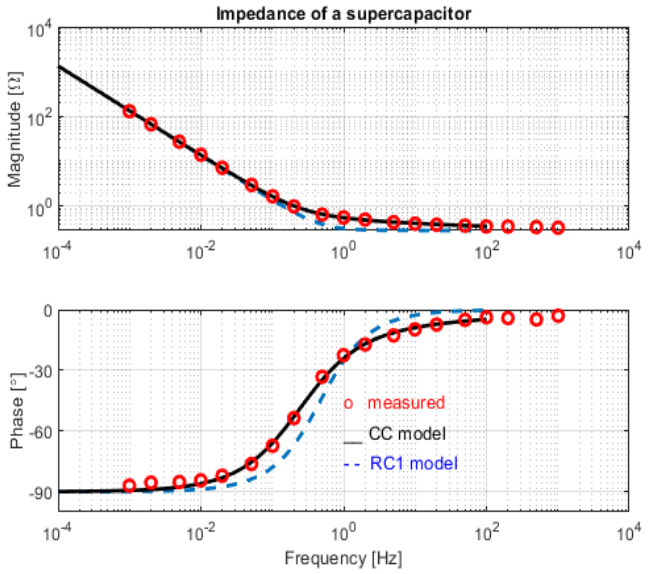

Fig. 5. Frequency characteristics of the impedance of the 1 F supercapacitor: measurement results – circles, fractional CC model – continuous line, RC1 model – dashed line

sented cases concern different technologies for manufacturing supercapacitors.

To verify the method of determining the parameters of supercapacitor impedance models, determined by the frequency method, a comparison of the voltage impulse responses of supercapacitors and simulations for their models with the same current excitation was made. Figure 6 shows the voltage responses of the supercapacitor and its RC1 and CC models to a current charge pulse of 5 s.

As already mentioned, the impulse responses of the CC model with parameters optimized for the frequency response differ slightly from the real responses. These differences are much greater for the RC1 model.

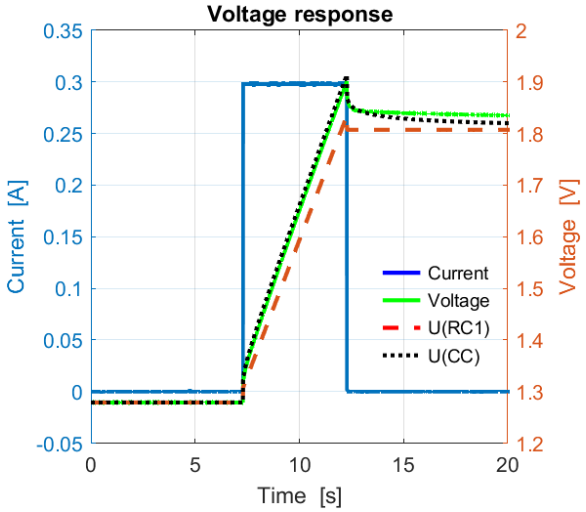

Fig. 6. Voltage response of a 3.3 F supercapacitor to 5 s wide current discharge pulse: real (green), RC1 model (red dashed) and CC model (black dotted)

3. DETERMINATION OF THE ENERGY EFFICIENCY OF SUPERCAPACITORS

The study of energy losses in supercapacitors conducted by the authors of the article concerned a selected representative load of supercapacitors in the energy storage system of an electric vehicle. It was assumed that the supercapacitors were excited by a pair of rectangular current pulses of the same duration and amplitudes, but with opposite polarities. They correspond to the braking-acceleration sequences and vice versa. The duration of a single pulse was assumed to be in the range of 3–10 s, and the break between them was 3–20 s. Figures 7 and 8 show examples of current and voltage waveforms of the supercapacitor. As mentioned, after current pulses the voltage of the supercapacitor still changes. This is related to the relaxation processes inside it and the resulting additional release of thermal energy. This means that energy losses last longer than the current pulses. However,

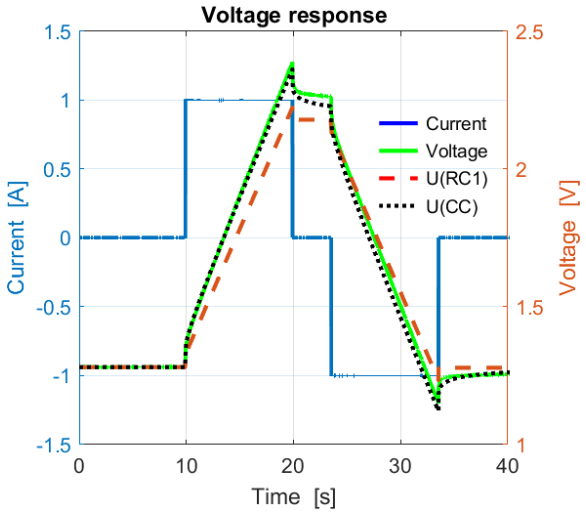

Fig. 7. Current forcing (blue) and voltage response of 1 F supercapacitor: real – green, RC1 model – red dashed, CC model – black dotted

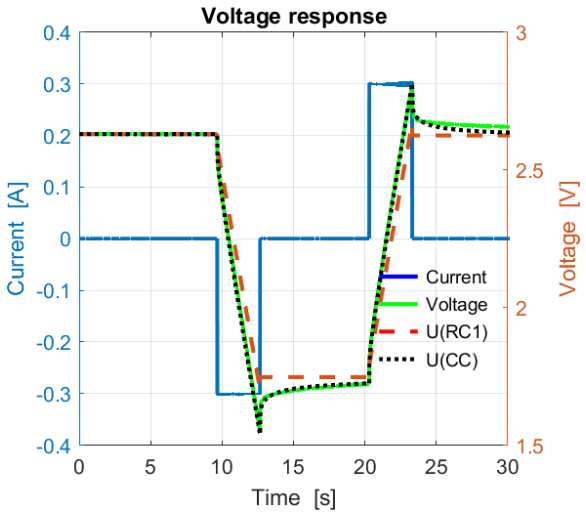

Fig. 8. Current forcing (blue) and voltage response of 1 F supercapacitor: real – green, RC1 model – red dashed, CC model – black dotted)

the balance of energy received and released by the supercapacitor during the current pulses facilitates the determination of the total thermal losses in the supercapacitor.

To determine the power efficiency of the supercapacitor, the value of energy supplied to the supercapacitor was assumed as

$$E_l = \int I_C U_C \, \mathrm{d}t \quad \text{for} \quad I_C > 0, \tag{18}$$

and the energy delivered from it to the storage system as

$$E_u = \int I_C U_C \, \mathrm{d}t \quad \text{for} \quad I_C < 0. \tag{19}$$

Current pulses $I_C(\mathrm{t})$ differ only in polarity, so the same electric charges are transferred. $U_C(\mathrm{t})$ is the voltage at the supercapacitor terminals. As a measure of electrical efficiency, the ratio used is

$$\eta = \frac{-E_u}{E_l}. \tag{20}$$

Let us assume the loss factor as

$$\xi = \frac{E_l + E_u}{E_l} = 1 - \eta. \tag{21}$$

The results of the loss factor ξ calculations for randomly selected supercapacitors of different capacities and from different manufacturers are presented in Table 1. These are results for the charging-discharging and discharging-charging sequences as shown in the graphs in Fig. 7 and Fig. 8. Table 1 compares the losses measured in the real supercapacitor and those calculated by simulation for the same excitations using the RC1 and CC models.

Table 1 shows that calculating losses based on the RC1 model leads to large underestimation. The errors in estimating losses based on the CC model are much smaller. The reasons for simulation errors based on the CC model were discussed earlier.

Table 1
The energy loss factor of supercapacitors for pulse pairs

Capacitance number	Pulses	Pulse width	Pause	Losses ξ measured	Losses ξ for RC1 model	Losses ξ for CC model
1 F, No. 1	−0.3 A +0.3 A	6 s	3 s	**26%**	8%	**20%**
	+0.3 A −0.3 A	3 s	5 s	**29%**	10%	**22%**
1 F, No. 3	−0.3 A +0.3 A	3 s	8 s	**13%**	3.5%	**13%**
	+0.3 A −0.3 A	6 s	5 s	**17%**	4%	**16%**
3.3 F, No. 3	−0.3 A +0.3 A	10 s	6 s	**8%**	2.5%	**9.5%**
	+0.3 A −0.3 A	5 s	20 s	**7.5%**	3%	**10%**
3.3 F, No. 8	−0.3 A +0.3 A	10 s	10 s	**6.5%**	1.2%	**7.5%**
	+0.3 A −0.3 A	10 s	5 s	**7%**	2%	**9%**
10 F, No. 3	−1 A +1 A	10 s	6 s	**11.5%**	4%	**12%**
	−1 A +1 A	10 s	3 s	**12.5%**	5%	**14%**
10 F, No. 5	−1 A +1 A	10 s	7 s	**6.5%**	1.8%	**7%**
	−1 A +1 A	10 s	5 s	**8%**	4.5%	**8.5%**

4. THE ISSUE OF DIFFERENT ESR DEFINITIONS

The energy losses of supercapacitors used in energy storage systems described so far are based on RC1 and CC models. They assume AC ESR values specified for 1 kHz. As mentioned, the DC ESR values are also given in a part of the technical data of supercapacitors. The IEC 62391-1: 2022 standard specifies the measurement conditions for both parameters. The authors of this paper presented comments on the measurement of capacitance according to the 2006 version of this standard [11]. According to the latest version of the standard [19], the AC ESR measurement does not raise any doubts. However, in the IEC 62391-1:2022 standard, the conditions for measuring capacitance and DC ESR are still presented in relation to the supercapacitor application classes. These classes are memory backup, energy storage, power, and instantaneous power. This distinction between measurement methods is omitted by manufacturers in their technical data. Moreover, their declarations regarding the application of the IEC standard are of little use if they do not contain additional information.

The IEC method of DC ESR measurement has a fundamental drawback. It assumes an approximation of the voltage response of the supercapacitor to a current step by a straight line, while in reality, this response is nonlinear (Fig. 1, Figs. 6–8). As mentioned, the CC model takes this feature into account by the presence of a fractional term of the impedance equation (11).

Due to this nonlinearity, some manufacturers also specify additional ESR measurement conditions that take it into account to some extent.

For example, to determine 'DC ESR_{IEC}' Ioxus assumes the voltage linearization based on its values after 1 s and 3 s from the start of the pulse. However, the technical data of this company's supercapacitors usually include 'DC $ESR_{10\,ms}$' values, which are based on the voltage change within 10 ms from the beginning of the discharging current pulse [27] – Fig. 9.

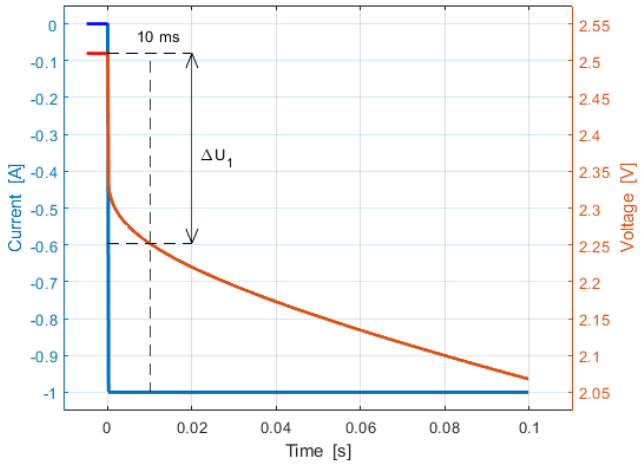

Fig. 9. Point of 'DC $ESR_{10\,ms}$' determining

The DC ESR value is calculated from the relationship

$$R_{\text{DC ESR}} = \frac{\Delta U}{I_A}, \tag{22}$$

where I_A is discharging current pulse amplitude and ΔU is voltage change. In this case $\Delta U = \Delta U_1$ (Fig. 9).

Other companies also use the 'DC $ESR_{10\,ms}$' measurement, e.g., LS Mitron [28]. Sometimes the basis of ESR determination is voltage change after some other time from the pulse start, e.g., 50 µs [29].

All the above methods are based on voltage changes in the initial period of a disturbance of the electrical state of the supercapacitor caused by a current pulse. Tests of voltage changes from the moment the disturbing impulse ends are also used. Skeleton bases the DC ESR measurement on the voltage change after 10 ms for 'DC 10 ms ESR' and after 1 s for 'DC 1s ESR' from the pulse end [30]. The voltage changes during this type of measurement are illustrated in Fig. 10. For 'DC 10 ms ESR' determined in equation (22) it should be assumed that $\Delta U = \Delta U_2$ while for 'DC 10 ms ESR' it should be assumed that $\Delta U = \Delta U_3$.

Skeleton also allows 'DC 10 ms ESR' measurement using the procedure with current pulse wave excitation [30]. Maxwell, on the other hand, uses an ESR measurement method based on its own six-step charge and discharge sequence [31].

In cases where AC ESR and DC ESR are given in technical data together, their ratio is considerably different. The authors of this paper measured the DC ESR by several methods and compared the simulation results when replacing the AC ESR in the RC1 model with the obtained values. The results for the 1 F

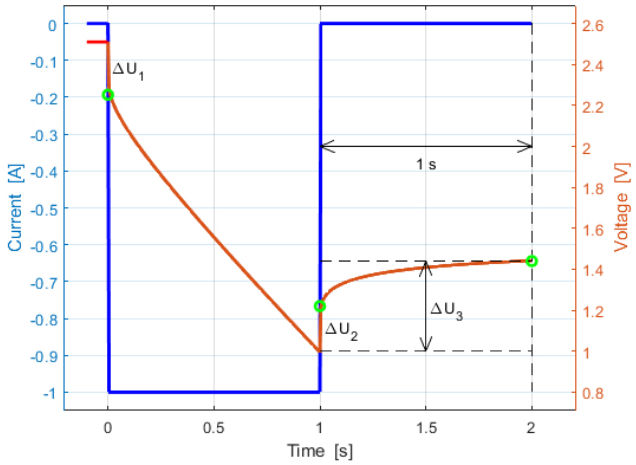

Fig. 10. Points of DC ESR determining by various methods

supercapacitor No. 3 for the discharge/charge pulse pair as in Table 1 are presented in Table 2.

Table 2

Energy losses in 1 F No. 3 supercapacitor for models with various ESR values

Measuring method	ESR	T	δ	$\frac{\xi \text{ for model}}{\xi \text{ measured}}$
AC ESR for 1 kHz	154 mΩ	–	–	0.26
DC ESR, 10 ms after pulse start	290 mΩ	–	–	0.48
DC ESR, 10 ms after pulse end	280 mΩ	–	–	0.47
DC ESR, 1 s after pulse end	470 mΩ	–	–	0.77
CC model parameters	154 mΩ	0.223 s	0.696	1.0

Replacing the AC ESR values in RC1 models with DC ESR values reduces the errors in estimating the real energy losses. In general, it can be stated that for the pulse cases covered by the studies described, the use of RC1 models leads to a significant underestimation of the value of these losses. The result for 'DC 1s ESR' presented in Table 2 is better but this parameter is rarely given in practice.

The problem of calculating energy losses in supercapacitors is additionally complicated by the increase in ESR values at low temperatures, but the self-heating of the supercapacitor as a result of this somewhat reduces the negative effects. The increase in ESR values due to the degradation of supercapacitors during their use is more important. Manufacturers try to solve the above problems by declaring that ESR values do not exceed certain limits.

As mentioned in the beginning, when the supercapacitor state of charge is prepared by the control system to supply or receive energy by a supercapacitor, it is done using a relatively small current. This is because the energy flow time between the supercapacitor and the main energy source is much longer than the energy flow time between the supercapacitor and the storage

load. For the tested 1 F No. 3 supercapacitor, a tenfold reduction of the current and the same extension of the pulse duration causes real losses and the CC model losses to be about 2.5%, while those calculated based on the RC1 model and AC ESR are 0.5%. Applying DC ESR leads to intermediate results.

5. CONCLUSIONS

Energy losses in supercapacitors significantly depend on the way they are charged and discharged. In energy storage systems, energy losses in supercapacitors are mainly related to the pulse energy exchange between them and the load. Supercapacitor manufacturers provide only the nominal capacitance and ESR of supercapacitors in their technical data. These are elements of the first-order RC model of the capacitor impedance. The article shows that attempts to calculate energy losses in supercapacitors used in energy storage devices conducted based on catalog ESR values and the first-order RC impedance model, generally lead to a significant underestimation of these losses. The solution to the problem may be a computer simulation using a fractional-order model of the supercapacitor impedance. A model of this type, based on the Cole-Cole relaxation equation, together with the simulation results of energy losses during pulse operation is presented in this paper.

It can also be stated that the ESR data can only be the basis for mutual comparison of energy losses when using supercapacitors from the same manufacturer. The thermal effects [32] and the effects of supercapacitor wear [33] should also be considered.

ACKNOWLEDGEMENTS

We would like to thank the Warsaw University of Technology for partial support of this work with a grant in the discipline of Automation, Electronics, Electrical Engineering, and Space Technologies entitled “Research on the energy efficiency of supercapacitors – proper selection of parameters in the energy storage”.

REFERENCES

[1] S. Sharma and P. Chand, “Supercapacitor and electrochemical techniques: A brief review,” *Res. Chem.*, vol. 5, p. 1000885, 2023, doi: 10.1016/j.rechem.2023.100885.

[2] J. Zhang, M. Gu, and X. Chen, “Supercapacitors for renewable energy applications: A review,” *Micro Nano Eng*, vol. 21, Dec. 2023, doi: 10.1016/j.mne.2023.100229.

[3] M. Lewandowski, M. Orzylowski, and M. Wieczorek, “Application of supercapacitors in electric traction storage systems,” *MATEC Web Conf.*, vol. 180, pp. 4–9, 2018, doi: 10.1051/matecconf/201818002002.

[4] M. Lewandowski and M. Orzylowski, “Novel Time Method of Identification of Fractional Model Parameters of Supercapacitor,” *Energies (Basel)*, vol. 13, no. 11, p. 2877, Jun. 2020, doi: 10.3390/en13112877.

[5] L. Shi and M.L. Crow, “Comparison of ultracapacitor electric circuit models,” *IEEE Power and Energy Society 2008 General Meeting: Conversion and Delivery of Electrical Energy in the 21st Century, PES*, Jun. 2008, doi: 10.1109/PES.2008.4596576.

[6] A. Sahin, M.E. Blaaberg, F. Snagwongwanich, “Modelling of Supercapacitors Based on Simplified Equivalent Circuit,” *CPSS Trans. Power Electron. Appl.*, vol. 6, no. 1, pp. 31–39, 2021.

[7] H. Miniguano, C. Fern, P. Zumel, and L. Antonio, “A General Parameter Identification Procedure Used for the Comparative Study of Supercapacitors Models,” *Energies (Basel)*, vol. 12, p. 1776, 2019, doi: 10.3390/en12091776.

[8] K.S. Cole and R.H. Cole, “Dispersion and absorption in dielectrics I. Alternating current characteristics,” *J. Chem. Phys.*, vol. 9, no. 4, pp. 341–351, 1941, doi: 10.1063/1.1750906.

[9] R.H. Cole and W. Davidson W., “Dielectric relaxation in glycerol, propylene glycol, and n-propanol,” *J. Chem Phys.*, vol. 19, no. 12, pp. 1484–1490, Dec. 1951.

[10] A. Dzieliński, D. Sierociuk, and G. Sarwas, “Some applications of fractional order calculus,” *Bull. Pol. Acad. Sci. Tech. Sci.*, vol. 58, no. 4, pp. 583–592, Dec. 2010, doi: 10.2478/v10175-010-0059-6.

[11] M. Lewandowski and M. Orzyłowski, “Fractional-order models: The case study of the supercapacitor capacitance measurement,” *Bull. Pol. Acad. Sci. Tech. Sci.*, vol. 65, no. 4, pp. 449–457, 2017, doi: 10.1515/bpasts-2017-0050.

[12] U. Mehta, R. Prasad, and K. Kothari, “Various Analytical Models for Supercapacitors: a Mathematical Study,” *Resour.-Effic. Technol.*, vol. 1, pp. 1–15, 2020, doi: 10.18799/24056537/2020/1/218.

[13] M. Lewandowski and M. Orzyłowski, *Wybrane zagadnienia modelowania i zastosowania superkondensatorów*. Warszawa: Oficyna Wydawnicza Politechniki Warszawskiej, 2021.

[14] A. Allagui, H. Benaoum, A.S. Elwakil, and M. Alshabi, “Non-Debye impedance and relaxation models for dissipative electrochemical capacitors,” *IEEE Trans. Electron Dev*ices, vol. 69, no. 10, pp. 5792–5799, Oct. 2022, doi: 10.1109/TED.2022.3197384.

[15] T.J. Freeborn, B. Maundy, and A.S. Elwakil, “Fractional-order models of supercapacitors, batteries and fuel cells: A survey,” *Mater. Renew. Sustain. Energy.*, vol. 4, no. 3, pp. 1–7, 2015, doi: 10.1007/s40243-015-0052-y.

[16] Q. Zhang and K. Wei, “A comparative study of fractional-order models for supercapacitors in electric vehicles,” *Int. J. Electrochem. Sci.*, vol. 19, no. 1, Jan. 2024, doi: 10.1016/j.ijoes.2023.100441.

[17] C.A. Monje, *Fractional-Order Systems and Controls, Fundamentals and Applications*. Springer London Dordrecht Heidelberg New York, 2010. doi: 10.1007/978-1-84996-335-0.

[18] A. Rufer, *Energy Storage: Systems and Components*, CRC Press, 2018.

[19] International Standard IEC 62391-1:2022 “Fixed electric double-layer capacitors for use in electronic equipment, Part 1: Generic Application,” International Electrotechnical Commission, Oct. 2022.

[20] J.L. Déjardin and J. Jadzyn, “Determination of the nonlinear dielectric increment in the Cole-Davidson model,” *J. Chem. Phys.*, vol. 125, no. 11, p. 114503, 2006, doi: 10.1063/1.2346378.

[21] R. Kopka, “Estimation of Supercapacitor Energy Storage Based on Fractional Differential Equations,” *Nanoscale Res. Lett.*, vol. 12, p. 636, 2017, doi: 10.1186/s11671-017-2396-y.

[22] J. Sung and C. Shin, “Recent studies on supercapacitors with next-generation structures,” *Micromachines*, vol. 11, p. 1125; Dec. 2020, doi: 10.3390/mi11121125.

[23] P. Galek, A. Slesinski, K. Fic, and J. Menzel, “Peculiar role of the electrolyte viscosity in the electrochemical capacitor perfor-

mance," *J. Mater. Chem. A Mater.*, vol. 9, no. 13, pp. 8644–8654, Apr. 2021, doi: 10.1039/d0ta11230e.

[24] L. Kexue and P. Jigen, "Laplace transform and fractional differential equations," *Appl. Math. Lett.*, vol. 24, no. 12, pp. 2019–2023, Dec. 2011, doi: 10.1016/j.aml.2011.05.035.

[25] J. Sabatier and C. Farges, "Initial value problems should not be associated to fractional model descriptions whatever the derivative definition used," *AIMS Math.*, vol. 6, no. 10, pp. 11318–11329, 2021, doi: 10.3934/math.2021657.

[26] X.D. Chen and I. Petras, "Fractional Order Control – A Tutorial," *Proceedings of 2009 American Control Conference*, pp. 1397–1411, 2009.

[27] IOXUS, "Representative Test Procedures for Customer Evaluations," no. 7–105, 2015. [Online] available at: https://www.rell power. com/ wp/wp-content/uploads/2015/07/Ioxus-Test-Procedures-for-Customer-Evaluations.pdf

[28] LS Mitron, "TEST METHOD 1) Capacitance 2) DC ESR 3) Leakage Current 4) Self-Discharge." [Online] available at: https://www.lsmaterials.co.kr/_common/download.asp?menucat=upYDsKYx&fname=fHTxgHXyfmj5kI4zg003g1cVeLUIsE

[29] CAP-XX, "GA109 / GA209 Supercapacitor," October, pp. 2–9, 2015. [Online] available at: https://www.cap-xx.com/wp-content/uploads/datasheets/CAP-XX-GA109-GA209-Datasheet.pdf

[30] Skeleton Technologies, "Instructions for Testing of Skeleton Technologies' Ultracapacitors," [Online] available at: https://www.skeletontech.com/downloads

[31] Maxwell, "Test Procedures for Capacitance, ESR, Leakage Current and Self-Discharge Characterizations of Ultracapacitorse," 2015.

[32] G. Xiong, A. Kundu, and T.S. Fisher, *Thermal Effects in Supercapacitors*. Springer, 2015, doi: 10.1007/978-3-319-20242-6.

[33] E. Pameté *et al.*, "The Many Deaths of Supercapacitors: Degradation, Aging, and Performance Fading," *Adv. Energy Mater.*, vol. 13, no. 29, p. 2301008, Aug. 2023, doi: 10.1002/aenm.202301008.